Analysis of the Magnetic Flux Distribution in a New Shifted Non-Segmented Grain Oriented AC Motor Magnetic Circuit

Guillaume Parent, R. Penin, J. Lecointe, J.F. Brudny, T. Belgrand

Analysis of the Magnetic Flux Distribution in a New Shifted Non Segmented Grain Oriented AC Motor Magnetic Circuit

G. Parent[1,2], R. Penin[1,2,3], J.P. Lecointe[1,2], J.F. Brudny[1,2], and T. Belgrand[3]
[1] Univ. Lille Nord de France, F-59000 Lille, France
[2] UArtois, LSEE, F-62400 Béthune, France
[3] ThyssenKrupp Electrical Steel, F-62330 Isbergues, France

This paper deals with a new AC electric motor magnetic circuit structure made of shifted non-segmented grain oriented steel laminations. The aim of the paper is to understand with a finite element approach the local distribution of the magnetic flux density inside shifted laminations as well as in the air-gaps between them. It is shown that the air-gap flux distribution is not trivial at all and very difficult to appreciate.

***Index Terms*—AC machine efficiency, finite element methods (FEMs), grain oriented electrical steel, magnetic cores.**

I. Introduction

USUALLY, most of the low and medium power AC electric rotating machine magnetic circuits are made of Non Oriented (NO) steel. Grain Oriented (GO) steel laminations, as for them, are used in transformer cores.

Nevertheless, recently, a new AC stator magnetic circuit, based on the stacking of shifted non-segmented GO sheets, has been developed [1][2]. Previous works showed that such a structure allows decreasing iron losses in the machine compared with stators made of NO sheets of same thickness [3]. This method has been applied to a 11 kW induction machine in order to make it more environment-friendly [4]. Indeed, its efficiency has been increased of 3% at full load compared with the same machine built with NO sheets magnetic circuit [3]. The emitted noise has also been reduced [5]. Hence, this kind of GO steel magnetic circuit may be included in a higher IE class. Moreover, in a certain way, this structure presents some similarities with transformer core corner joints [6].

In such configurations, the b magnetic flux density in the magnetic circuit of the machine has to pass from one lamination to another in order to satisfy the principle of energy minimization. Hence, b flows both in the planes of the magnetic sheets and in a direction perpendicular to those planes. That 3D distribution is really particular and specific and so required to be studied. In this paper, the authors show that the path thus taken by b is not trivial at all. Moreover, due to the very small thickness of the air-gaps between laminations, measuring b experimentally is quite a difficult task. Hence, using numerical methods, such as the Finite Element (FE) method, is the most appropriate approach for the understanding of this kind of phenomena.

In the first part of this paper, the studied device is presented and the authors show with a FE simulation how the magnetic flux distribution on the latter is complex. Moreover, FE results are strengthned with experimental results. The second part consists in several FE results showing which parameters influence the magnetic flux density distribution in the struture. The last part, as for it, is a results discussion in which the authors explain the reasons of the 3D flux distribution.

II. Studied setup - Particularities of the magnetic flux density distribution

A. Non-segmented shifted GO steel sheets stack

The studied structure is an annular yoke made of GO laminations whose Rolling Directions (RDs) are shifted from each other by a constant β angle (Fig. 1). An unidirectional excitation is provided by a winding regularly laid out around the yoke and supplied by a sinusoidal current. This structure seems very simple to analyze at first glance. Nevertheless, contrary to a classical NO steel sheet stack in which the magnetic flux density is homogeneous and identical in every single sheet, the latter, in this particular stack, follow rather the lamination whose RD is the most adapted to its circulation - minimizating the magnetic energy - and, depending on the reluctance of the air-gaps, crosses the latters [7].

Hence, studying this annular structure excited with an uniform pulsating magnetic field is an important step for the understanding of the phenomena occuring in GO magnetic circuit of AC machines excited with a rotating magnetic field. The paper relates about a structure made of GO steel sheets of 0.35 mm thickness and the study is limited to the case $\beta = 90°$.

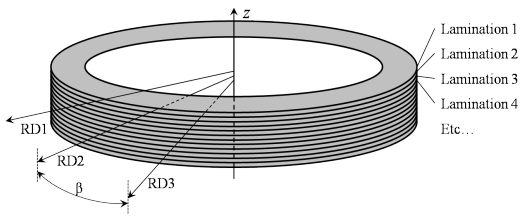

Fig. 1. Yoke composed of shifted laminations

B. Finite Element model

In order to analyze the magnetic flux distribution in the studied structure, a FE simulation of a stack of annular GO

steel sheets such as the one presented in Fig. 1 is performed using the code GETDP [8]. The internal radius, the external radius and the thickness of each sheet are 100 mm, 81.5 mm and 0.35 mm respectively. Moreover, the model takes into account both the insulation and the interlaminar thicknesses by including a 5 µm air-gap between each lamination.

With such a ratio between the sheets and the air-gaps thickness, it is obvious that modeling a stack made of hundreds of laminations, like in a real stator, is not an option. Indeed, such cases would lead to extremely high computation time problems, or even unsolvable problems. Hence, in order to get accurate results with descent computation times, the model is made of a number of sheets chosen as follows : at a given β angle, only three times the number of sheets necessary to cover a full permutation are modelled. As an example, for $\beta = 90°$, a full permutation is covered by two sheets, so six sheets are modeled and the fields are analyzed in the two ones situated in the middle of the stack in order to avoid the influence of the borders on the flux distribution. Note that for $\beta = 90°$ it is also possible to take advantages of symetries and so only model two sheets.

The anisotropy of the GO sheets is defined by three directions : the Rolling Direction (RD), the Transverse Direction (TD) and the Normal Direction (ND). The first two directions are included into the plane of the sheets, while the third one is normal to that plane (Fig. 4). Hence, the relation between the magnetic flux density and the magnetic field can be expressed as follows:

$$\begin{pmatrix} b_{RD} \\ b_{TD} \\ b_{ND} \end{pmatrix} = \begin{pmatrix} \mu_{RD} & 0 & 0 \\ 0 & \mu_{TD} & 0 \\ 0 & 0 & \mu_{ND} \end{pmatrix} \cdot \begin{pmatrix} h_{RD} \\ h_{TD} \\ h_{ND} \end{pmatrix} \quad (1)$$

In (1), each magnetic permeability μ_{RD}, μ_{TD} and μ_{ND} is a function of the magnetic field so that saturation is taken into account (Fig. 2). The first magnetization $b(h)$ curves related to the RD and the TD are determined by standardised Epstein frame test. On the other hand, the curve related to the ND is obtained by use of a specific test bench [9] and the values are conform to those found in the literature [10]. Relation (1) allows taking into account the magnetic characteristics only in the main directions. This is a simple method to get hints about the field behaviour, but appropriate enough for this study. Furthermore, very few other approaches are available. Moreover, a more realistic model would mean integrate the behaviour of domain walls in the material [11] which is something not available at present time. Finally, in order to get results as valid as possible, every simulations are performed with both scalar and vector magnetic potentials formulations [12].

C. Results

The results of the FE simulation of the studied stack in the case of $\beta = 90°$ are presented in Fig. 3 and in Fig. 4. The latter shows the air gap magnetic flux distribution in the case of lamination 2 (whose RD is RD2) is on top of lamination 1.

As expected, b is concentrated in the sheets that are best adapted to its circulation (Fig. 3). Nevertheless, it is noticeable that the flux distribution in the air-gap is not homogeneous. Indeed, in Fig. 4, three zones can be highlighted.

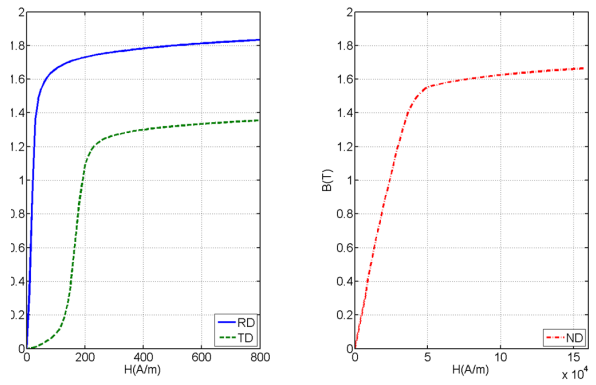

Fig. 2. $b(h)$ curves in RD, TD and ND

The first one shows a flux concentration toward the external border of the structure. Actually, this zone represents the area where the magnetic flux density passes through the air gap, leaving the RD of a lamination to reach the RD of another lamination. That phenomenon was expected. On the other hand, the fact that this zone is concentrated toward the external border of the structure is noticeable. This phenomenon is quite easy to explain actually. Indeed, once the magnetic flux follow the RD of a lamination, it tends to follow it as long as possible before crossing the air-gap. Thus, the best place for the flux to cross pass from one sheet to another is situated at 45°, *ie* $\frac{\beta}{2}$, from the RDs. But due to the annular shape of the sheets, the flux meets the border of the laters before 45°, leading to a concentration on the external border.

The second and third zones are more unexpected. Indeed, in the zone 2 close to the central hole, there is a concentration of flux density similar to the first zone, but with an opposed direction. This internal border is rather unusual. Finaly, there is almost no flux in the zone 3.

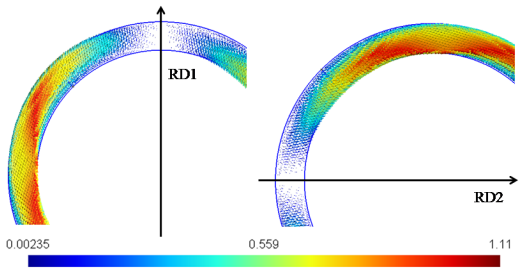

Fig. 3. Distribution of b in stacked laminations

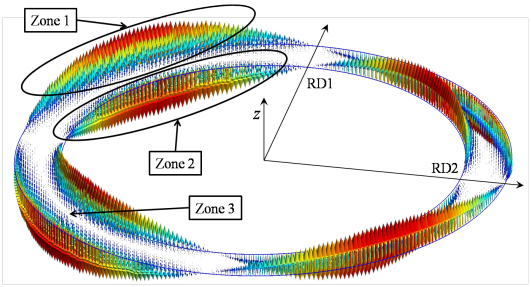

Fig. 4. Distribution of b in the air-gap between two stacked laminations

TABLE I
EXPERIMENTAL VALUES

Sensor	1	2	3	4	5	6	7	8	9
Sensor Voltage (µV)	34.2	31.2	124	41.3	15.5	79.6	92.8	19.8	68
B (mT)	18.1	16.5	66.1	21.9	82.3	42.3	49.2	10.5	36.1
Phase lag (°)	Ref	-172.7	-179.1	-176	-5.3	0.1	-10.4	-169.1	-73.8

It is also interesting to underline that the flux density in the air-gap presents, spatially, a sinusoidal waveform. Fig. 5 presents this distribution along 360° close to the two borders (zones 1 and 2) and in the middle (zone 3) of the structure.

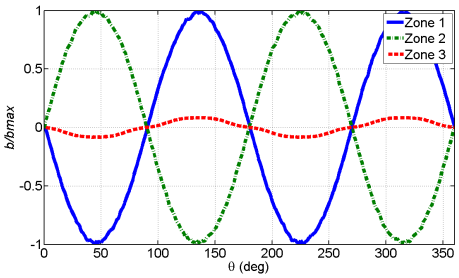

Fig. 5. Distribution of b in the air-gap

D. Experimental validation

Since the flux density distribution is different than expected, an experiment on a real stack excited as stated in section II-A has been performed. The frequency of the excitation is set at 50 Hz and the global value of the b magnetic flux density is 0.7 T. Nine wounded sensors (three turns of 4 mm denoted 1 to 9 in Fig. 6) have been placed in three zones: three of them in the RD of a lamination whereas the last six ones are seperated into two groups of three at 45° on both sides of the RD. They make it possible to measure the magnetic flux density close to the borders and in the middle of the lamination. Table I shows that the three sensors noted 7, 8 and 9 positioned along the RD measure low flux amplitudes, which is in accordance with the results of the FE simulation (Fig. 4). Moreover, the voltages measured by sensors 1 and 3 are higher than sensor 2. The same comment can be made about sensors 4 and 6 compared with sensor 5. It can be pointed out that, despite the fact that sensors 1, 2, 3 and 4, 5, 6 are located symmetrically with RD, differences concerning the amplitudes occur. Those differences come from the sensors themselves. Indeed, they are manually wounded and then stuck between the sheets. Hence, their shapes may not exactly be the same at first and also may have been modified during the sheets clamping process. The results are prefectly in accordance with the FE simultation results when it comes to phases. Indeed, the signals measured by sensors 1 and 3 are phase-opposited as well as the signals measured by sensors 4 and 6.

III. PARAMETERS INFLUENCING THE FLUX DENSITY DISTRIBUTION

Several parameters have been modified in order to understand their impact on the magnetic flux density distribution in the structure.

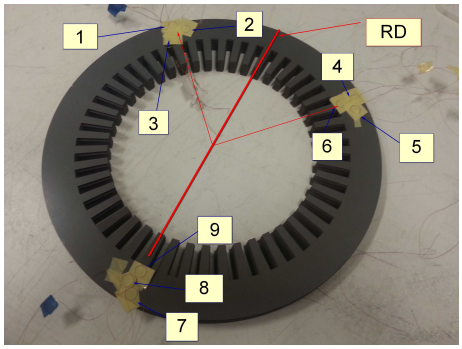

Fig. 6. Position of the 9 sensors between 2 sheets

A. Impact of the internal radius

The internal radius of the rings has been reduced, the external radius being unchanged. That influences the distribution of b in the sheets and in the air gap, as shown in Fig. 7. The zone 1 has moved from the external border to be closer from the central hole. The zone 2, where the flux is almost null is still present. The zone 3 is really more reduced. It shows that the central hole has a major rule for the flux distribution : as the hole size is reduced, the zone 3 is not so important.

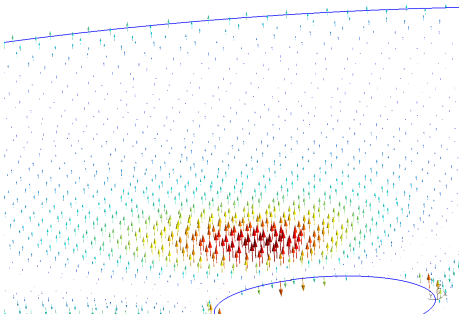

Fig. 7. Distribution of b in the air gap with a reduced central hole

B. Impact of the air-gap thickness

The air-gap thickness does not change the path taken by the flux and the three zones defined previously are still present. Nevertheless, the values of the magnetic flux density are, of course, impacted. Indeed, the thinner the air-gap is, the less reluctant it is and so the flux present in the laminations can cross it more easily when it has to turn toward the RD.

C. Impact of the saturation

The FE simulation results presented in previous sections involved a stack magnetization level in the linear part of the constitutive law (1). Taking into account a higher magnetization level of the stack, *ie* more saturated sheets, doesn't change the double path of the flux density observed in Fig. 4. Indeed, each one of the three zones previously highlighted is present in unsaturated as well as saturated cases. The saturation of the laminations on the flux density distribution in the air-gap is presented in Fig. 8. Instead of being purely sinusoidal, the waveforms are classically deformed by the saturation.

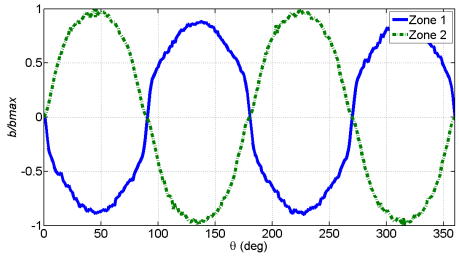

Fig. 8. Distribution of b in the air-gap

IV. Results and discussion

The section III has shown what the influent parameters are. Let us analyse the two zones, keeping in mind that the flux "tries" to follow the RD as longest as possible. Concerning the first zone, the flux tends, as it has been sensed in section II, to be in the RD. Then, it goes down or up through the air gap to the RD of the adjacent sheet. That explains well the distribution of b in the air gap between the RD of two nearby sheets, as shown in Fig. 9 with the dotted blue path. This figure , where the ring has a small internal radius allows understanding the flux distribution. The central hole acts as a buttress for the flux, which can not continue into the RD. As a consequence, although passing through the TD of the same sheet, it passes the air gap for being in the RD of the next sheet. When the internal radius is close to the external

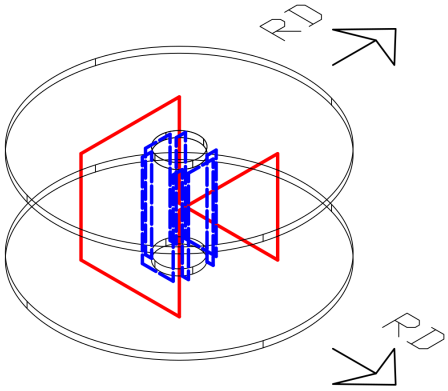

Fig. 9. Scheme of the flux path with a small central hole

radius, the flux goes from one lamination to another in order to follow the less reluctant path. Fig. 10 shows such a path, which goes from the internal hole to the external border. That scheme also explains why b in the zone 1 and in the zone 3 are phased-opposed. Moreover, it justifies the zone 2 of the air-gap, where there is almost no flux crossing.

V. Conclusion

This paper highlights a particular flux distribution in a simple device made of GO shifted steel sheets. That distribution shown by FE results has been also verified with experiments. Several FE simulations, for which some parameters have been changed, allows understanding the origin of the flux distribution. The authors explain it finally with simplified schemes. Such a study allows well understanding the flux distribution in new magnetic circuits made of GO non-segmented

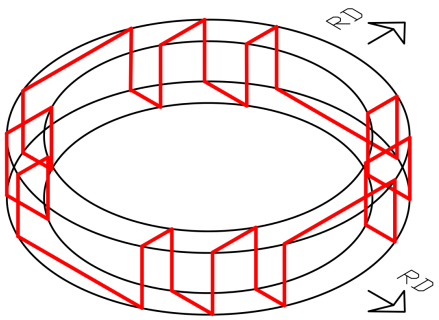

Fig. 10. Scheme of the flux path with a large central hole

laminations. Moreover, these conclusions can be very usefull in order to calculate the losses in such structures as well as they allow finding explanations on how the Maxwell forces and the magnetostriction forces occur between the sheets and in the magnetic circuit respectively.

Acknowledgment

This work is supported by MEDEE program supervised by the French national technological research cluster on electrical machine efficiency increase. This program, including ThyssenKrupp Electrical Steel, is sponsored by the region Nord Pas-de-Calais (France), the French ministry and the European founds (FEDER).

References

[1] J.-F. Brudny, B. Cassoret, R. Lemaître, and J.-N. Vincent, "Magnetic core and use of magnetic core for electrical machines," WO Patent Application WO 2009/030 779 A1, 03 12, 2009.

[2] ——, "Magnetic core and use of magnetic core for electrical machines," US Patent Application US 2011/0 260 574 A1, 10 27, 2011.

[3] S. Lopez, B. Cassoret, J. Brudny, L. Lefebvre, and J. Vincent, "Grain oriented steel assembly characterization for the development of high efficiency ac rotating electrical machines," *Magnetics, IEEE Transactions on*, vol. 45, no. 10, pp. 4161 –4164, oct. 2009.

[4] W. Boughanmi, J. Manata, D. Roger, T. Jacq, and F. Streiff, "Life cycle assessment of a three-phase electrical machine in continuous operation," *Electric Power Applications, IET*, vol. 6, no. 5, pp. 277–285, may 2012.

[5] C. Demian, B. Cassoret, J.-F. Brudny, and T. Belgrand, "Ac magnetic circuits using nonsegmented shifted grain oriented electrical steel sheets: Impact on induction machine magnetic noise," *Magnetics, IEEE Transactions on*, vol. 48, no. 4, pp. 1409 –1412, april 2012.

[6] N. Hihat, E. Napieralska-Juszczak, J. Lecointe, J. Sykulski, and K. Komeza, "Equivalent permeability of step-lap joints of transformer cores: Computational and experimental considerations," *Magnetics, IEEE Transactions on*, vol. 47, no. 1, pp. 244–251, jan. 2011.

[7] H. Pfutzner, K. Futschik, P. Hamberger, and A. M., "Concept for more correct iron loss measurements considering path length dynamics," in *12th international workshop on 1&2 dimensional magnetic measurement and testing*, 2012.

[8] P. Dular, C. Geuzaine, F. Henrotte, and W. Legros, "A general environment for the treatment of discrete problems and its application to the finite element method," *IEEE Transactions on Magnetics*, vol. 34, no. 5, pp. 3395–3398, Sep. 1998.

[9] N. Hihat, K. Komeza, E. Napieralska Juszczak, and J. Lecointe, "Experimental and numerical characterization of magnetically anisotropic laminations in the direction normal to their surface," *Magnetics, IEEE Transactions on*, vol. 47, no. 11, pp. 4517 –4522, nov. 2011.

[10] H. Pfutzner, C. Bengtsson, T. Booth, F. Loffler, and K. Gramm, "Three-dimensional flux distributions in transformer cores as a function of package design," vol. 30, no. 5, pp. 2713–2727, 1994.

[11] A. Ebrahimi and A. J. Moses, "Correlation between normal flux transfer from lamination to lamination during the magnetization process with static domain structures in grain oriented 3no. 10, pp. 6265–6267, 1991.

[12] A. Bossavit, "Whitney forms: a class of finite elements for three-dimensional computations in electromagnetism," *IEE Proc. A*, vol. 135, no. 8, pp. 493–500, Nov. 1988.